https://doi.org/10.3311/PPee.20827

Periodica Polytechnica Electrical Engineering and Computer Science, 67(1), pp. 83–94, 2023

Impact of Dimensions, Apertures and Terminals on Stray Inductance of the Laminated Busbar

Aravind Venugopal[1], Femi Robert[1]*

[1] Department of Electrical and Electronics Engineering, College of Engineering and Technology, SRM Institute of Science and Technology, SRM Nagar, Potheri, 603203 Kattankulathur, Chengalpattu, Tamil Nadu, India
* Corresponding author, e-mail: femir@srmist.edu.in

Received: 15 July 2022, Accepted: 21 October 2022, Published online: 13 December 2022

Abstract

This paper presents a systematic investigation of the impact of physical parameters such as dimensions, apertures and terminals, on the busbar inductance. A planar laminated busbar with copper conductors and a polyamide insulator is studied using a 3D FEM (Finite Element Modelling) based simulation software. The impact of dimensions such as conductor length, width and thickness, depth of insulator, the effects of aperture number, size, position and connection terminals on the busbar inductance are examined. The magnetic flux density, current density involved and its dependence on the self and mutual inductance of the laminated busbar is analyzed. Laminated busbars provided lower inductance with decreased conductor length, thickness, aperture diameter and depth of insulator. Also, the increased width of the busbar is of the essence for the design of a low inductance busbar. Low inductance laminated busbars are highly beneficial in power converters, powertrain inverters in electric vehicles, photovoltaic converters.

Keywords

aperture, electric vehicle, FEM, laminated busbar, stray inductance

1 Introduction

Busbars have been an integral part of the power distribution precinct for decades as they provide much better electrical and mechanical performance than conventional cabling systems. Cabling systems possess some crucial caveats such as decreased mechanical strength, lower thermal efficiency, in comparison to busbars. Busbars provide smaller conductor thickness for a specific current rating than cables as well as better heat dissipation since the air circulation around the conductor is much larger [1–3]. Its other advantages include lower stray inductance and reduced EMI (Electromagnetic Interference) issues than cables [4]. However, standard busbar systems, have higher stray inductance than laminated busbars, leading to voltage spikes on power electronic components during turn-OFF transients, thereby increasing the overall losses [5, 6]. In comparison, they require considerable space and material, which causes practical issues in the system. Laminated busbars provide compact connections with ample mechanical support while keeping the overall system footprint comparatively low. High power applications such as electric vehicles, motor drives and photovoltaic inverters commonly use laminated busbars [7–9]. Laminated busbars are essential in electric vehicle design since the size and weight of components are crucial constraints in electric transportation [10]. They provide lower stray inductance and higher power density, thus making it inevitable for pivotal components such as power converters and inverters used in electric vehicles [11–13]. Hence, they are beneficial in the design and implementation of traction inverters, battery banks, onboard battery charging systems and fast-charging stations [14]. With increasing power requirements and the need for advanced power electronic systems for safety, comfort, convenience and performance features, implementation of laminated busbars proves to be one of the most efficient schemes in the electric vehicle industry [15]. Also, efficient and reliable electric vehicles are the future in the transportation sector since they have much lesser environmental impacts while being economically viable [16].

Over the past few decades, laminated busbar inductance has been a subject of importance to many researchers [17–19]. Caponet et al. [20] focused on a low inductance busbar design with regards to electromagnetic compatibility and have proposed expressions for internal as well as external inductances. However, Wang et al. [21] clearly

Cite this article as: Venugopal, A., Robert, F. "Impact of Dimensions, Apertures and Terminals on Stray Inductance of the Laminated Busbar", Periodica Polytechnica Electrical Engineering and Computer Science, 67(1), pp. 83–94, 2023. https://doi.org/10.3311/PPee.20827

states that these expressions are often deceptive and unreliable based on FEM-based simulation results since the initial studies did not consider the impact of physical dimensions on the busbar. Also, practical busbars depend on apertures and terminals to provide the necessities of the application. Apertures are essentially perforations in the structure which facilitate the connection of components on the laminated busbar. Hence apertures and terminals play a significant role in low inductance busbar designs. Besides, there aren't many studies that extensively concentrate on the effect of physical parameters, that affect the stray inductance of the laminated busbar.

Also, the selection of conductor and insulator materials is a crucial factor in busbar design. Commonly used materials for conductors are copper, aluminum, copper alloys, whereas for insulators, usually Nomex, Mylar, Kapton are used [22]. The conductor size of the busbar depends on the material used and its threshold temperature rise allowance, for meeting the required current rating of the application [17]. Insulator size, and material selection also impacts the parasitic parameters such as stray inductances and also the thermal efficiency of the busbar [7]. Increased stray inductance in the busbar causes several issues among which, the occurrence of surge voltages across components in the busbar during transients, is of utmost importance [23]. The voltage surges can cause significant problems to the power electronic components used in the busbar, their longevity and can even lead to a dielectric breakdown in the laminated busbar, affecting overall system reliability [9]. Lower stray inductances are crucial in an efficient laminated busbar as it reduces the overall losses in the system [24].

This work discusses the impacts of the various physical parameters on the inductance of the laminated busbar, in detail. It focusses mainly on the effects of physical dimensions, apertures and terminals of the laminated busbar on its inductance. Analyses are performed in the 3D FEM software Ansys Maxwell. Section 2 discusses the structure of the basic planar laminated busbar used. Section 3 showcases the dependence of busbar inductance on its dimensions. Sections 4 and 5 present the impacts of apertures and terminals on the busbar inductance, respectively. Section 6 represents the conclusions, providing the inferences from the analysis.

2 Basic laminated busbar structure

Laminated busbars are essentially current-carrying conductors separated by an insulation layer with connection arrangements for specific applications. The conducting layers are tightly pressed together with the insulating material in between. In Ansys Maxwell, the insulating boundary condition is applied on the surfaces between the conductor and insulator. Analyses are performed in the magnetostatic solution type with a curvilinear meshing of size resolution. An adaptive type solver setup with a maximum of 10 passes and a percent error of unity is used. The simulation model used is a basic planar laminated busbar with copper (Cu) conductors and a polyamide (PA) insulator. Table 1 showcases the crucial properties of the materials used in this laminated busbar.

The basic laminated busbar structure with dimensions, l = 150 mm, w = 100 mm, t = 3 mm and d = 1 mm is considered for the study, where l represents the length, w represents the width, t represents the thickness of the busbar conductor and d represents the depth of the insulator. The dimensions of the laminated busbar are chosen so that it would be ideal for the traction inverter of an electric car with currents ranging up to 100 A. Fig. 1 represents the basic laminated busbar structure used for the investigation.

FEM simulations are performed on the busbar structure from Fig. 1 for analyzing the effect of different parameters on the laminated busbar inductance. The different simulation cases used for analysis are represented in Table 2.

The dimensions of the laminated busbar including the width, length and thickness of the conductors as well as the depth of the insulator are varied to study their dependence on the busbar inductance. Simulations suggested that for

Table 1 Properties of materials used in the busbar

Material	Density (g cm^{-3})	Resistivity (Ω m)	Thermal conductivity (W m^{-1} K^{-1})	Specific heat (J kg^{-1} K^{-1})
Copper	8.96	1.72×10^{-8}	401	385
Polyamide	1.14	1.4×10^{14}	0.2	1.5×10^{6}

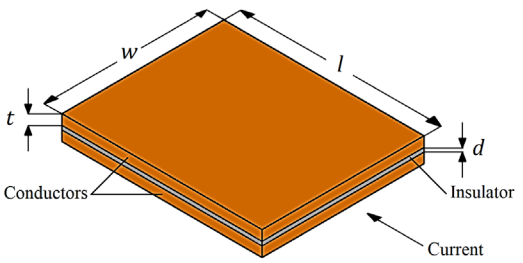

Fig. 1 Laminated busbar structure with dimensions l, w, d and t

Table 2 Simulation cases used for analysis

Sl. No.	Simulation cases	Parameters
1.	Varying dimensions	w, l, t, d
2.	Varying apertures	aperture diameter, number, position
3.	Varying terminals	terminal position

low inductance busbar designs, the laminated busbar width should be higher and l, t, d should be lower. The impact of conductor length on the self and mutual inductances of the laminated busbar is also studied. The number, position and diameter of the apertures are also varied on the laminated busbar structure to study their influence on the stray inductance. Furthermore, the terminal positions on the busbar structure are varied to investigate the dependence of terminals on the inductance. Magnetic flux densities and current densities are plotted and studied for analyzing the dependence of the physical parameters on the stray inductance of the laminated busbar.

3 Impact of dimensions

The dimensions such as length, width, height and thickness of the busbar conductors influence their overall inductance. The characteristic impedance of the busbar, Z is given by [17]:

$$Z = \sqrt{\frac{L}{C}}, \tag{1}$$

where L and C represents the stray inductance and capacitance of the busbar, respectively. For planar laminated busbars with two conductors, the expressions for inductances are formulated by applying Maxwell's equations. These equations are given by [17]:

$$L_s = 2l\left(\log\left(\frac{2l}{w+t}\right)+0.5+0.2235\left(\frac{w+t}{l}\right)\right)\times 10^{-7}, \tag{2}$$

$$L_m = 2l\left(\log\left(\frac{2l}{d}\right)-1+\frac{d}{l}\right)\times 10^{-7}, \tag{3}$$

where L_s and L_m represent the self-inductance of conductors and mutual inductance between the conductors, respectively. Furthermore, the total equivalent inductance, L_{total} is given by [22]:

$$L_{\text{total}} = \frac{\mu_0 l}{w}\left(d+\frac{2t}{3}\right), \tag{4}$$

$$L_{\text{total}} = 2\left(L_s - L_m\right), \tag{5}$$

where μ_0 represents the permeability of vacuum. From Eq. (5), it is clear that the reduction of the total stray inductance of the busbar is attainable by decreasing the self and mutual inductances of the busbar. Increased mutual inductance leads to the cancellation of magnetic flux lines and consequently, reduces the effective inductance. Also, Eq. (4) suggests that the total inductance is directly proportional to the length and inversely proportional to the width of the laminated busbar conductors. Thus, the physical dimensions play a crucial role in determining the overall stray inductance of the busbar. Current excitation of 10 A is applied along the width of the busbar conductors for analysis. The region around the busbar structure is considered as air. Fig. 2 represents the self and mutual inductances of the planar laminated busbar over the variation of length, width, thickness of the conductor and depth of the insulator.

In Fig. 2 (a), width of the busbar is varied from 100 mm to 190 mm while keeping values of l, t and d constant. Fig. 2 (a) indicates that the increased width of the busbar conductors significantly aids in reducing the inductances of the busbar. In Fig. 2 (b), busbar length is varied from 150 mm to 240 mm while keeping the values of w, t, d constant. Thus, it is evident that the inductance significantly increases with increase in the busbar conductor length. In Fig. 2 (c), the conductor thickness is varied from 3 mm to 7.5 mm keeping the values of l, w, d constant. Thus, it is clear that the inductance increases with increase in the thickness of the busbar conductor. In Fig. 2 (d), depth of the insulator is varied from 1 mm to 5.5 mm, keeping the values of l, w, t constant. It is evident that the busbar inductance increases with increase in insulator depth. Hence, conductors with reduced lengths, thicknesses, increased widths and reduced insulator depth are essential in low inductance busbar design. Furthermore, Fig. 3

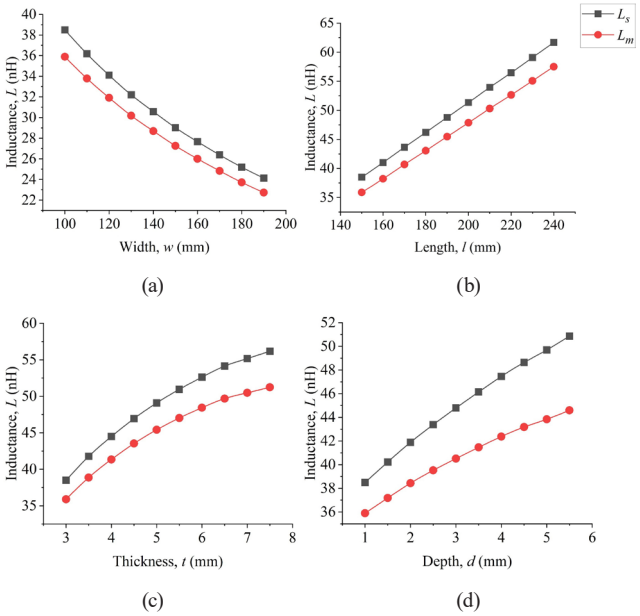

Fig. 2 Inductance variation with dimensions, (a) L vs w; (b) L vs l; (c) L vs t; (d) L vs d

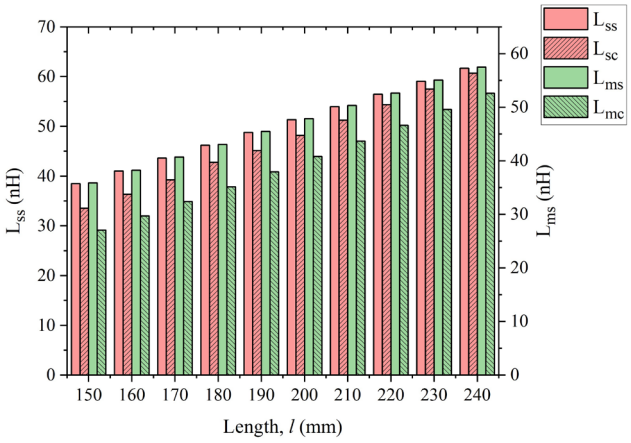

Fig. 3 Self and mutual inductances of the busbar as a function of length

showcases the comparison between simulation and calculation values of inductances for variation in lengths of busbar conductors.

L_{ss} and L_{ms} represent the simulated self, mutual inductances, respectively and L_{sc} and L_{mc} represent the calculated self, mutual inductances, respectively. Fig. 3 suggests that the difference in self and mutual inductances decreases with increase in the length of the laminated busbar conductors. Furthermore, busbar inductance is dependent on the ratio of conductor width to the depth of the insulator in between the conductors. Table 3 represents the variation in busbar inductance as a function of *w/d* ratio.

Table 3 indicates that the ratio *w/d* should be as high as possible for the design of a low inductance busbar. Thus, to reduce the inductance, the busbar width should be increased while keeping the depth of the insulator to a minimum value, so that it can withstand the operating voltage of the application.

4 Impact of apertures

Apertures are inevitable in practical laminated busbars since they are used to connect different components such as capacitors, power electronic switches, used in the system. Besides, they can increase the busbar thermal efficiency while decreasing the material requirement and thereby the cost of the system, if used judiciously.

Table 3 Dependence of busbar inductance on *w/d* ratio

Width, *w* (mm)	Depth, *d* (mm)	*w/d*	L_s (nH)	L_m (nH)
300	3	100	16.4247	15.5320
250	3.5	71.43	21.5941	20.4046
200	4	50	28.2598	26.6451
150	4.5	33.33	37.2249	34.9098
100	5	20	49.0865	45.4150

4.1 Influence of aperture size and number

The number, position and diameter of the apertures significantly affect the magnetic flux density and current density in the laminated busbar conductors. To study this electromagnetic dependence, FEM simulation is performed using the magnetostatic solver in Ansys Maxwell. A direct current of 10 A passed through the busbar conductors produces the static magnetic field. The field solutions acquired from simulations obey the following Maxwell's equations:

$$\nabla \times \vec{\boldsymbol{H}} = \vec{\boldsymbol{J}}, \tag{6}$$

$$\nabla \cdot \vec{\boldsymbol{B}} = 0, \tag{7}$$

where $\vec{\boldsymbol{H}}$, $\vec{\boldsymbol{J}}$ and $\vec{\boldsymbol{B}}$ represents magnetic field strength, current density and magnetic flux density, respectively. Fig. 4 represents magnetic flux density and current density as a function of varying aperture diameter on the laminated busbar surface.

Fig. 4 (a)–(d) represents the laminated busbar with aperture diameters of 40 mm, 55 mm, 70 mm and 85 mm, respectively. Table 4 gives the maximum values of busbar magnetic flux density and current density concerning this aperture diameter variation, with fixed *l*, *w*, *d* and *t*.

Table 4 suggests that the progressive increase in aperture diameter causes a corresponding increase in magnetic flux density and current density. Also, from Fig. 4 (b) and (c), it is clear that the magnetic flux density and current density increases substantially as the aperture diameter increases from 70 mm to 85 mm in comparison with the same for Fig. 4 (a) and (b). The dimension of the apertures with respect to the laminated busbar dimensions is a contributing factor to this phenomenon. That is, as the aperture reaches towards the edges of the busbar in Fig. 4 (b) and (c), current crowding at those edges, causes increased non-uniformity in current distribution, thereby increasing the current density. Similarly, the magnetic coupling between the conductors of the busbar is larger towards the point where the conductor surfaces are closer to each other. Thus, the impedances on the currents flowing at the edges of the busbar is much smaller in comparison. The increase in aperture diameter increases the magnetic flux density and current density in the laminated

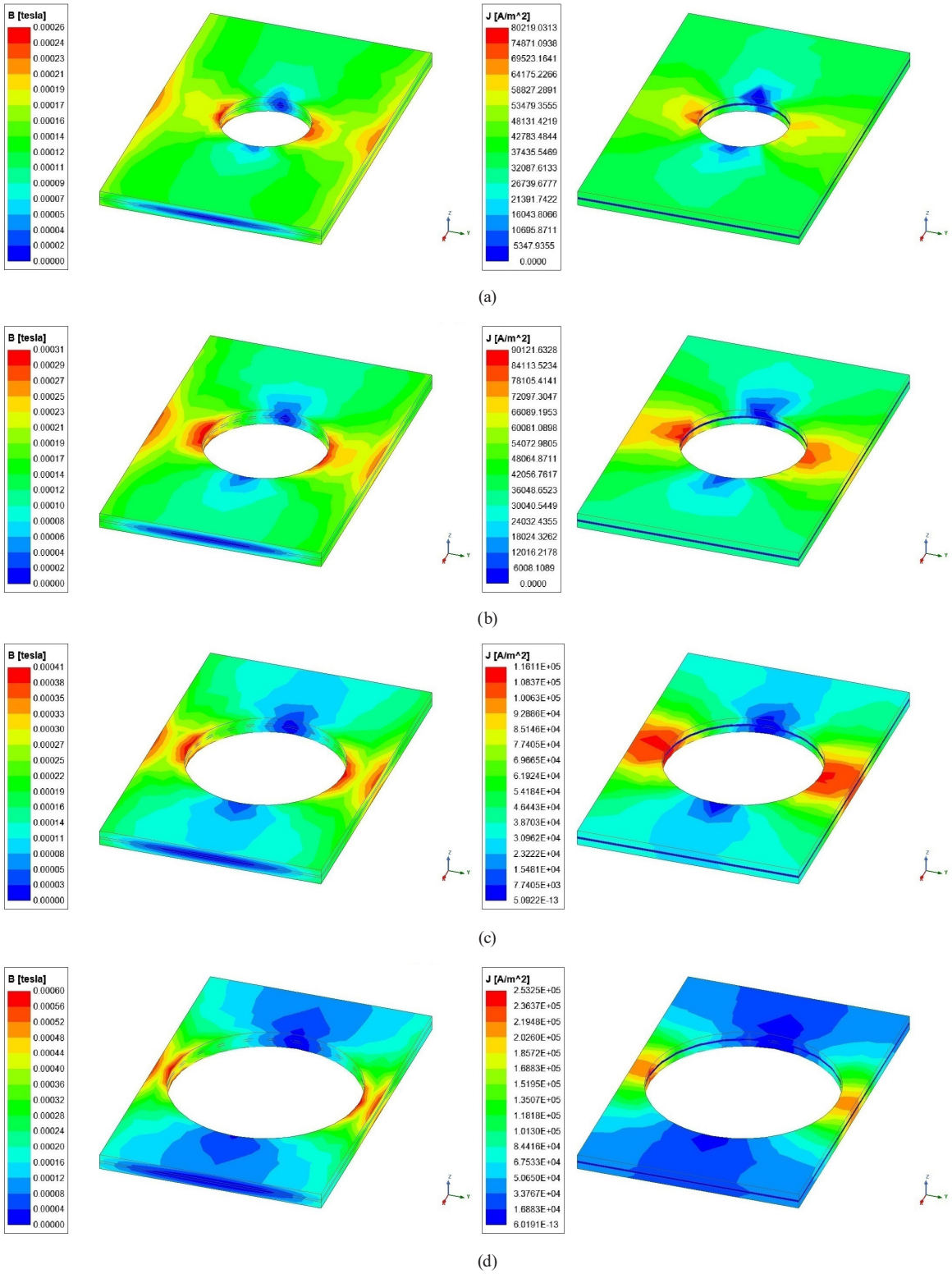

Fig. 4 ***B*** and ***J*** variations with aperture diameter (A_d); (a) A_d = 40 mm; (b) A_d = 55 mm; (c) A_d = 70 mm; (d) A_d = 80 mm

busbar. Thus, the current distribution in the busbar conductors gets even more unbalanced and increases the stray inductance. Fig. 5 depicts the increase in busbar inductance with an increase in aperture diameter.

Busbar conductors could have a better thermal convection effect with the reduction in the overall magnetic field, by having uniform current distribution [25]. In most practical applications, such as inverters, laminated busbars

Table 4 Values of ***B*** and ***J*** with aperture diameter variation *z*

Aperture diameter, A_d (mm)	Magnetic flux density, ***B*** (Tesla)	Current density, ***J*** (A/mm^2)
40	2.60×10^{-4}	0.0802
55	3.10×10^{-4}	0.0901
70	4.10×10^{-4}	0.1161
85	8.50×10^{-4}	0.2533

have multiple apertures to accommodate several components on the busbar. Busbar inductance undergoes variation due to deviation in the distribution of current density and magnetic flux density on the busbar. Fig. 6 represents the effect of the number and size of apertures on current density and magnetic flux density of the laminated busbar.

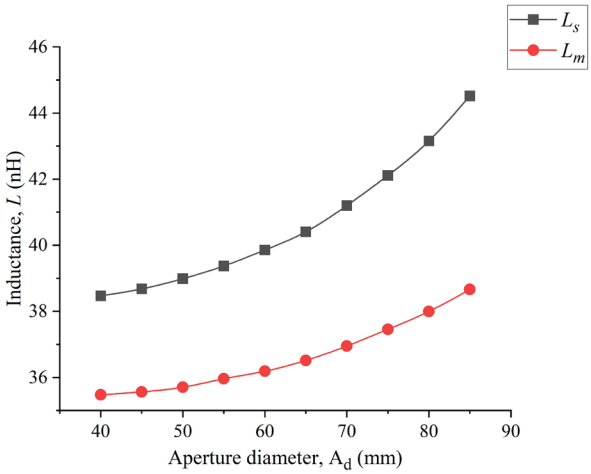

Fig. 5 Inductance variations with aperture diameter

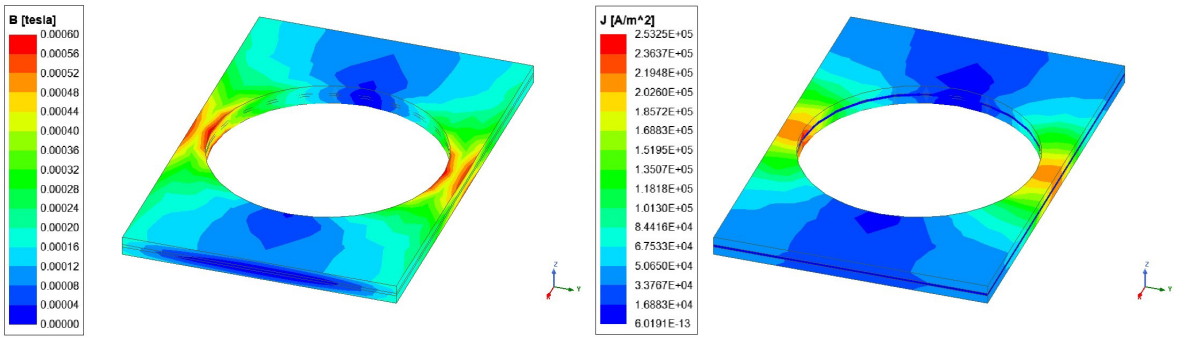

(a)

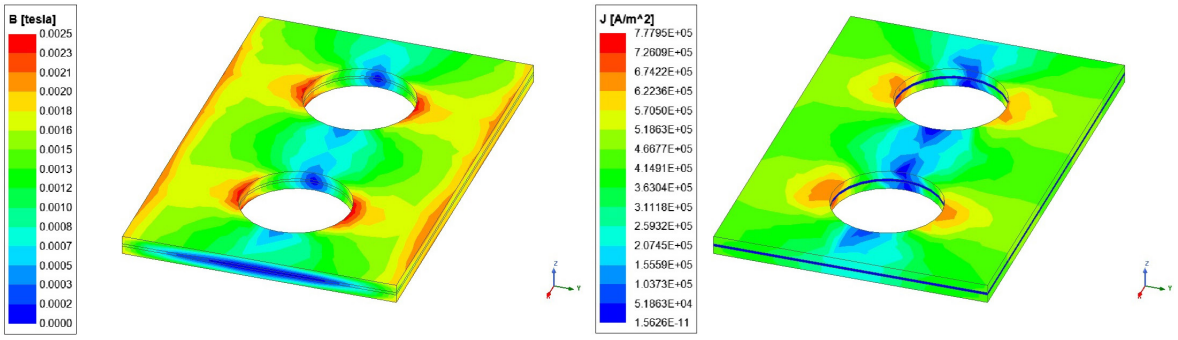

(b)

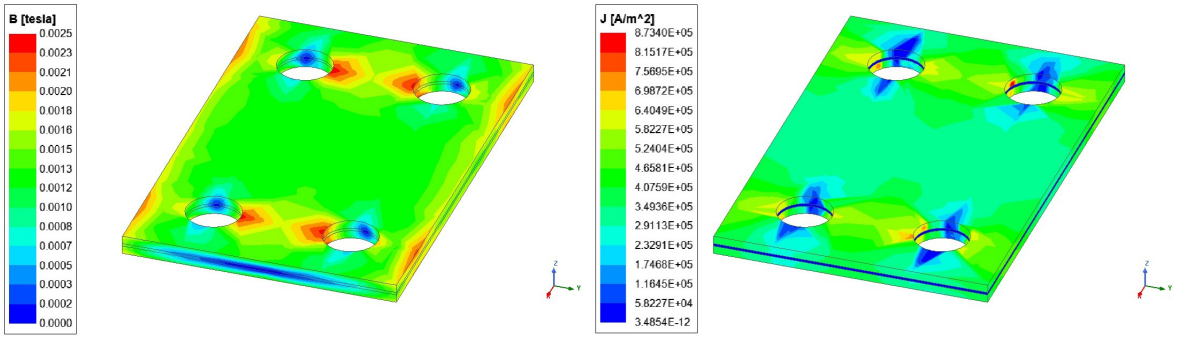

(c)

Fig. 6 ***B*** and ***J*** variations with the multiple apertures on the busbar; (a) b_1, A_d = 80 mm; (b) b_2, A_d = 40 mm; (c) b_3, A_d = 20 mm

Fig. 6 (a)–(c) represents the topologies, b_1, b_2 and b_3 of the laminated busbar, simulated with different aperture number and size for analysis. Busbar inductance decreases over the topologies since aperture diameter is decreasing. Reduction of aperture diameter allows accommodation of an increased number of apertures on the busbar. Table 5 represents the maximum values of magnetic flux density and current density with varying aperture number and diameter.

From Table 5, it is clear that the difference in magnetic flux density and current density values for the busbar topologies b_1, b_2 is more substantial than that of b_2, b_3, since the difference in the aperture number between the topologies b_2 and b_3 is twice that of the topologies b_1 and b_2. Also, the difference in aperture diameter for b_2 and b_3 is half that of topologies b_1 and b_2. Due to the decreasing current density, the current distribution in the structure gets more uniform in comparison, thereby decreasing the self and mutual inductance values of the laminated busbar. Fig. 7 represents the variation of inductance, with aperture diameter (A_d) and number of apertures (A_n) on the laminated busbar.

From Fig. 7, it is clear that the busbar topology b_2 is the most optimized topology in terms of reduced inductance. Topology b_2 has an aperture diameter of 40 mm with an aperture number of two. This combination aids

Table 5 ***B*** and ***J*** values as a function of number, diameter of apertures

Busbar topology	Aperture number, A_n	Aperture diameter, A_d (mm)	***B*** (Tesla)	***J*** (A/mm^2)
b_1	1	80	5.30×10^{-4}	0.1751
b_2	2	40	2.60×10^{-4}	0.0907
b_3	4	20	2.50×10^{-4}	0.0873

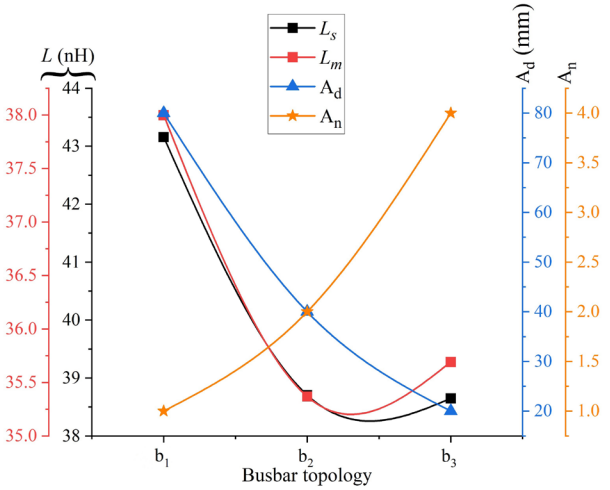

Fig. 7 Busbar inductance as a function of aperture number and diameter

b_2 in achieving the lowest overall inductance among the other topologies. Also, the reduction in the aperture diameter has a more prominent effect on the laminated busbar inductance than number of apertures. Also, the variation in laminated busbar inductance is minimal over topologies when total area of the apertures on the busbar surface remains the same. To study this aspect, two more busbar topologies bb_1 and bb_2 are simulated to acquire the inductances, magnetic flux density and the current density involved. Fig. 8 represents the magnetic flux densities and current densities of both the topologies.

Fig. 8 (a) represents the busbar bb_1 which has four apertures, each with an aperture diameter of 40 mm and Fig. 8 (b) shows the busbar bb_2 that has an aperture diameter of 80 mm. Aperture number on bb_2 is kept as one so that the total area of apertures for both topologies are the same. The variation in values of maximum magnetic flux density over the topologies is minimal, while the current density variation is relatively significant. As the self and mutual inductances of the topologies depend mostly on the busbar current density alone, the differences in L_s and L_m values among the topologies would be small. Fig. 9 represents the values of these self and mutual inductances for both the busbar topologies.

Fig. 9 indicates that the difference in self and mutual inductances for the busbar topologies are nominal. Also, the error percentages for the differences in self and mutual inductances among the topologies are under 2.6% and 1.9%, respectively. This indicates that the difference in laminated busbar inductance over busbar topologies is minimal if the aperture area remains the same among the topologies. Therefore, it is evident that aperture radius and size are crucial factors in low inductance laminated busbar design since the component connections on the laminated busbar depend on it.

4.2 Influence of aperture position

The position of apertures on the laminated busbar influences its inductance. Aperture position (A_p), specified as (x, y) coordinates in millimeters for the aperture center, is varied to analyze the resulting deviation in busbar inductance with the aperture diameter value fixed at 40 mm. Fig. 10 shows the busbar with apertures at different positions, as well as the magnetic flux density and current density involved.

Table 6 represents the maximum values of magnetic flux density and current density for variation in the position of aperture in the laminated busbar. From Table 6, it is

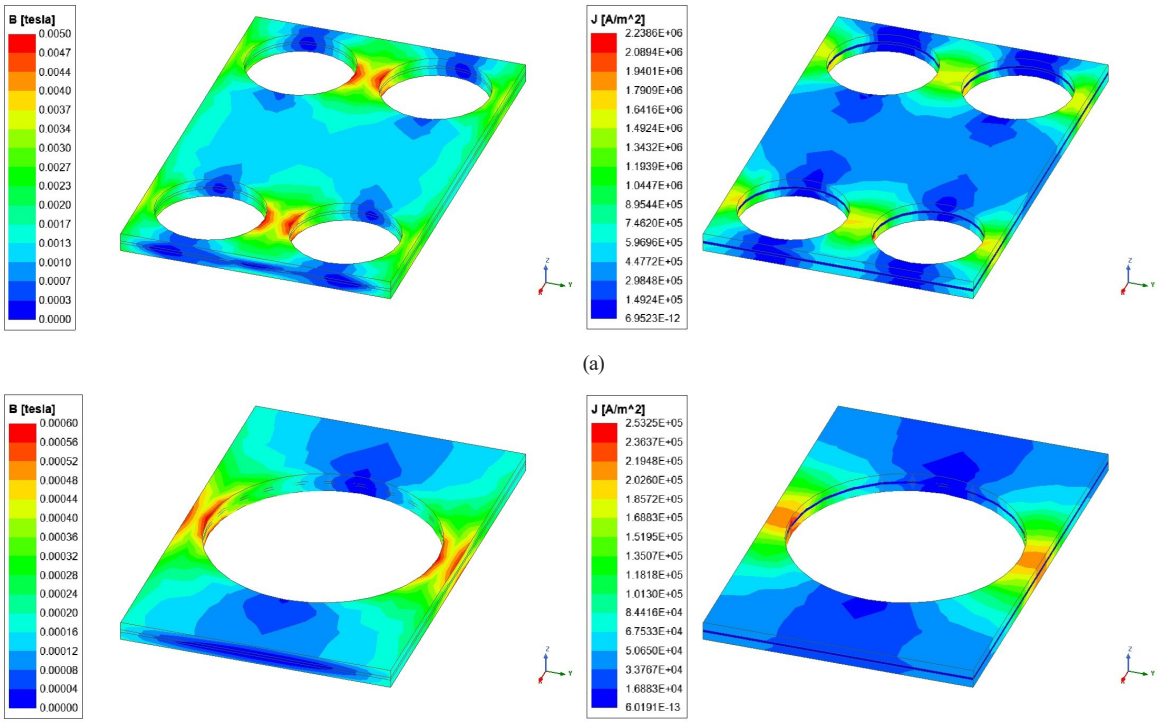

Fig. 8 Busbar **B** and **J** with varying A_d, A_n; (a) bb_1, A_d = 40 mm; (b) bb_2, A_d = 80 mm

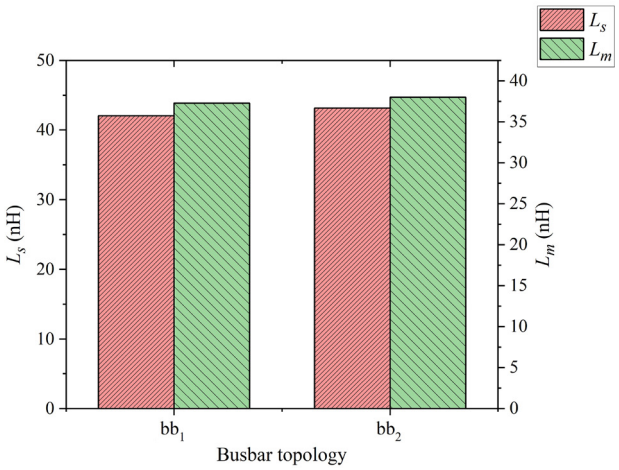

Fig. 9 Inductance variations of busbar topologies

clear that there is a considerable decrease in the magnetic flux density and current density values for even an incremental, moderate change in the position of the aperture.

Besides, Fig. 10 (a), (b) indicates that, as the aperture is close to the edges of the busbar, current density increases, the current distribution gets more non-uniform and increases the inductance. Thus, the symmetry of apertures on the laminated busbar leads to a better distribution of current and hence controls the stray inductance. Fig. 11 represents the self and mutual inductances as a function of the aperture position on the laminated busbar surface.

From Fig. 11, the dependence of the aperture position on busbar inductance is evident. Thus, the change in aperture position leads to significant variation in the inductance.

5 Impact of terminals

As with the case of apertures, the physical parameters concerning terminal connections have a sizeable influence on the magnetic flux density and the current density of the laminated busbar and thereby its inductance. Fig. 12 (a)–(c) represents the magnetic flux density and current density on busbar topologies, b_a, b_b and b_c, with terminals at different positions.

From Fig. 12, it is evident that the position of the terminals on the laminated busbar affects the magnetic flux density, current density, the current distribution and thereby the busbar inductance. Symmetrical terminal connections improve the current distribution, thereby reducing the inductance. Fig. 13 represents the variation of self and mutual inductances for the busbar topologies b_a, b_b and b_c.

Fig. 13 suggests that the inductances are most optimized in the busbar topology b_a. From Fig. 12 (a), in topology b_a, the busbar terminals are overlapping each other, leading to higher mutual inductance among the conductors. Thus, total inductance of the laminated busbar reduces, as per Eq. (5).

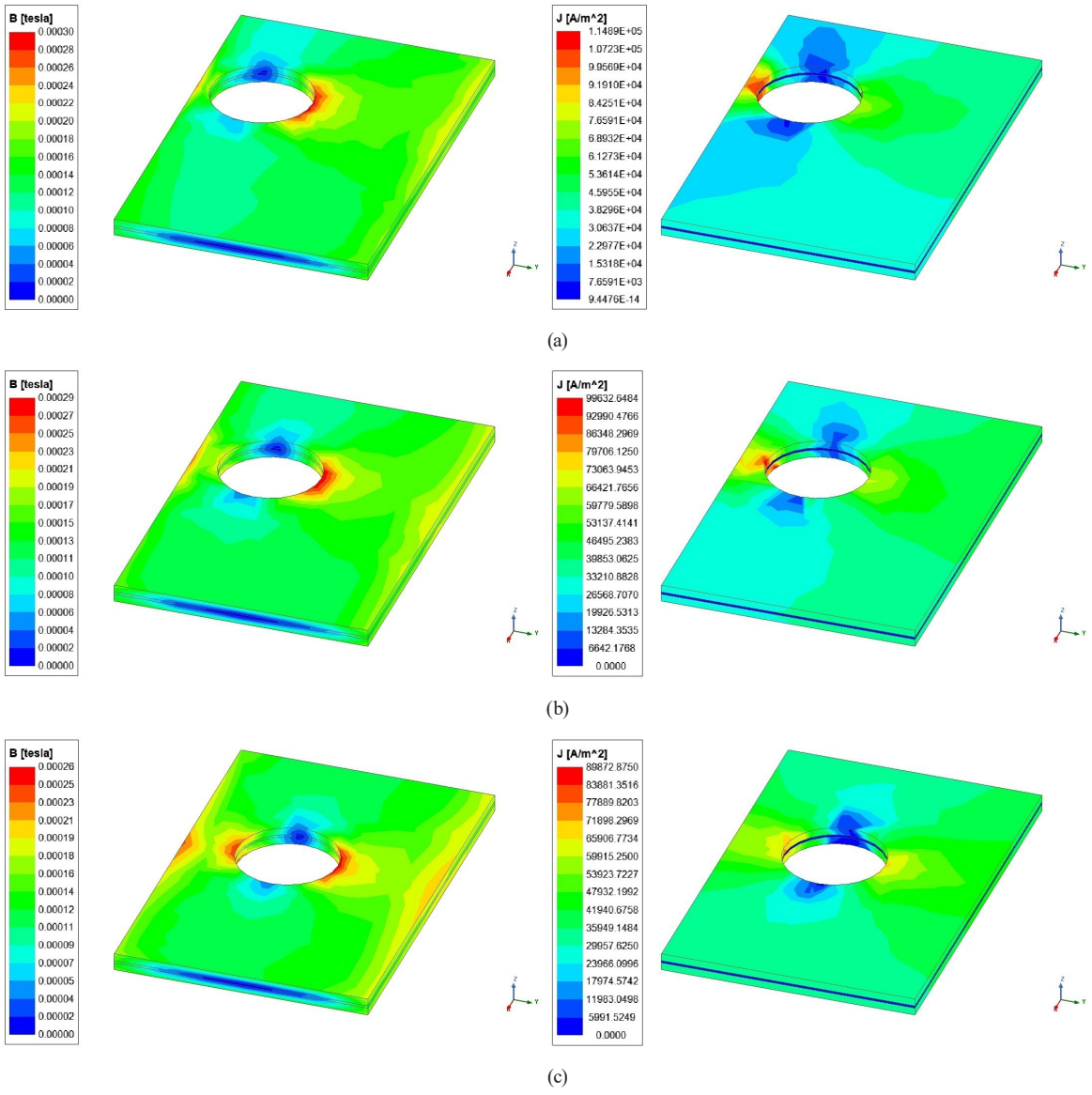

Fig. 10 ***B*** and ***J*** variation with aperture position; (a) A_p = (50, 25); (b) A_p = (55, 30); (c) A_p = (60, 40)

Table 6 ***B*** and ***J*** values concerning the change in aperture position

Aperture position, A_p (x, y) (mm)	***B*** (Tesla)	***J*** (A/mm^2)
(50, 25)	3.00×10^{-4}	0.1149
(55, 30)	2.90×10^{-4}	0.0996
(65, 40)	2.60×10^{-4}	0.0898

6 Conclusions

This paper presents a comprehensive study on the impact of physical parameters on the laminated busbar inductance. Inductance plays a vital role which influences the impedance of the busbar, thereby reducing the overall losses. It is inferred that, for low inductance busbar designs, thinner, wider conductors with decreased length and insulator thickness are necessary. Apertures and terminals on the

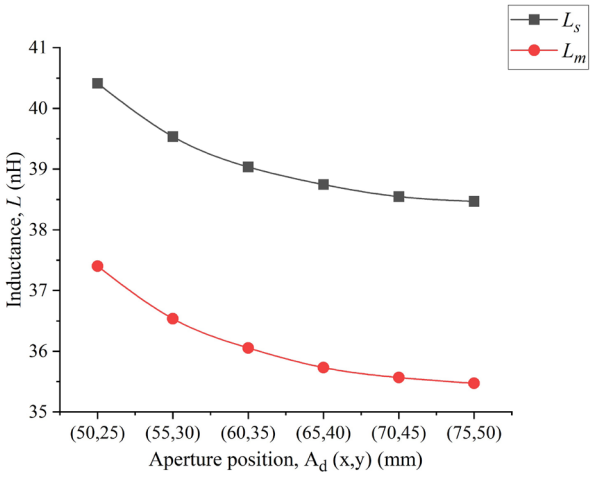

Fig. 11 Inductance variation with aperture position

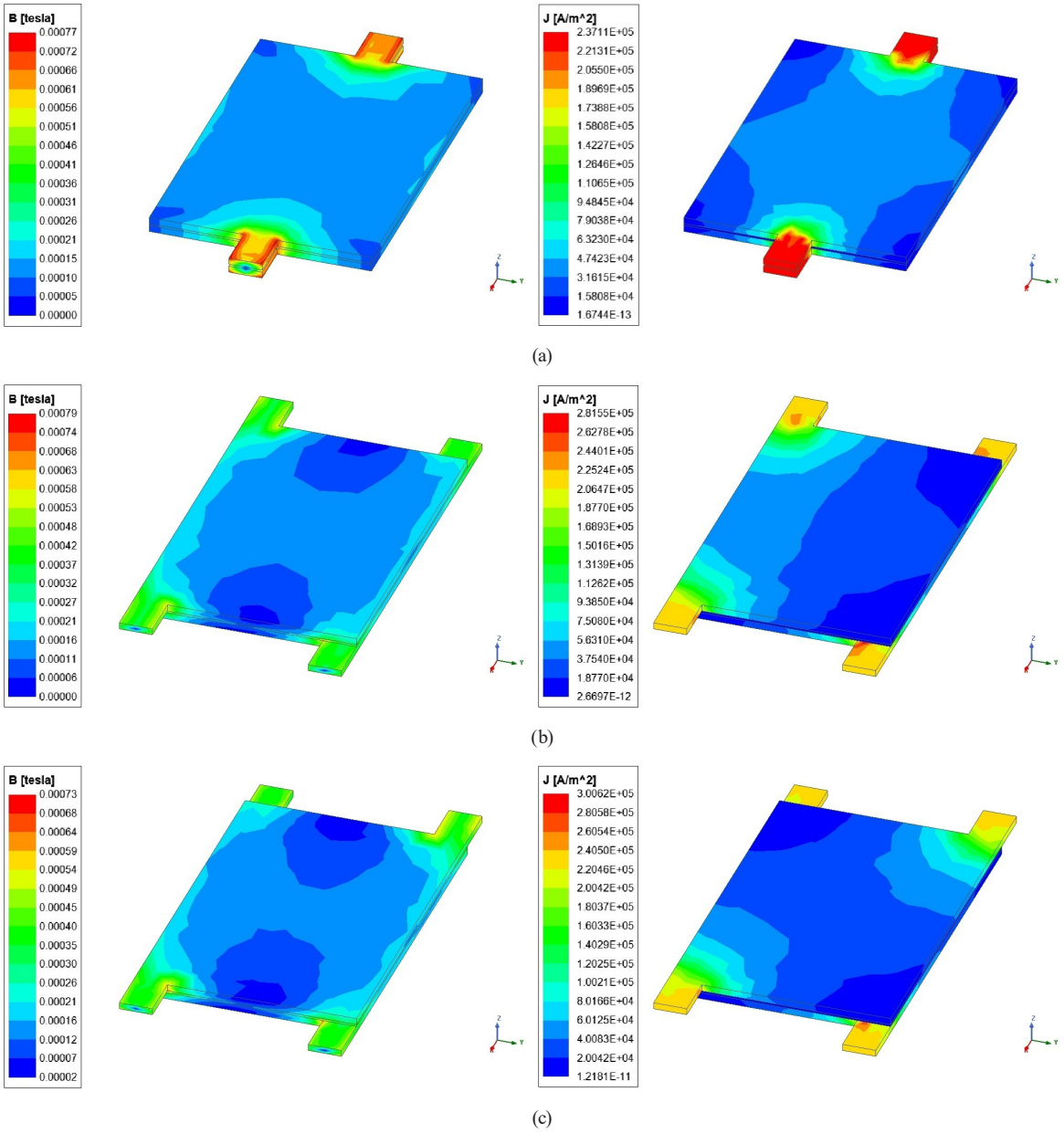

Fig. 12 ***B*** and ***J*** variation for busbar topologies with different terminal positions; (a) b_a; (b) b_b; (c) b_c

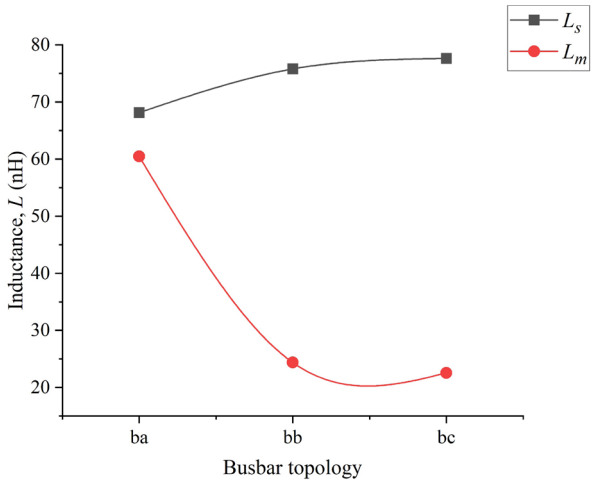

Fig. 13 Inductance variation for busbar topologies b_a, b_b, b_c

laminated busbar are of importance too, when it comes to low inductance busbar design. Inductance increases with an increase in aperture number as well as diameter on the laminated busbar structure. The variation in aperture and terminal positions on the structure also significantly affects the laminated busbar inductance. The optimal configuration of laminated busbar dimensions among the topologies, for the lowest possible inductance, is with l, w, d, t as 150 mm, 190 mm, 1 mm, 3 mm, respectively, and an aperture diameter of 40 mm. Simulations indicate that the magnetic flux density and current density are directly proportional to the busbar inductance since they can cause unbalanced current distribution on the laminated busbar. The symmetrical connection of terminals reduces the

laminated busbar inductance by improving the current distribution. The results and inferences from this study would be beneficial in low inductance laminated busbar design for medium and high power applications such as electric vehicle battery chargers, inverters and converters.

Acknowledgement

This work is part of SRMIST Selective Excellence Research Initiative-2021: "DCFCEVB".

References

[1] Schmerda, R. F. "Busbars", In: Webster, J. G. (ed.) Wiley Encyclopedia of Electrical and Electronics Engineering, John Wiley & Sons, Inc., 1999, pp. 624–634. ISBN 9780471346081 https://doi.org/10.1002/047134608X.W6101

[2] Petrášová, I., Karban, P., Pánek, D., Šroubová, L. "Shape and Topology Optimization of High Power Converter Busbar", In: 19th International Conference Computational Problems of Electrical Engineering, Banska Stiavnica, Slovakia, 2018, pp. 1–4. ISBN 978-1-5386-7896-1 https://doi.org/10.1109/CPEE.2018.8506702

[3] Schanan, J. L., Clavel, E., Roudet, J. "Modeling of low inductive connections: the planar busbar structure", In: Proceedings of 1994 IEEE Industry Applications Society Annual Meeting, Denver, CO, USA, 1994, pp. 1246–1250. ISBN 0-7803-1993-1 https://doi.org/10.1109/ias.1994.377556

[4] Zhang, X., Zhang, H., Yu, R.-W., Tan, G.-J. "Planar bus bar optimum design in high-power converters based on FEM analysis", In: The 2nd International Symposium on Power Electronics for Distributed Generation Systems, Hefei, China, 2010, pp. 167–170. ISBN 978-1-4244-5669-7 https://doi.org/10.1109/PEDG.2010.5545908

[5] Wang, Z., Chen, G. "Study on planar busbar regarding stray inductance minimization and oscillation suppression for high power converter", In: 2009 International Conference on Sustainable Power Generation and Supply, Nanjing, China, 2009, pp. 1–7. ISBN 978-1-4244-4934-7 https://doi.org/10.1109/SUPERGEN.2009.5347993

[6] Mitsui, K., Wada, K. "Design of Bus Bar Structures in Power Converter Circuit Considering Both Parasitic Inductance and AC Resistance", In: 2019 10th International Conference on Power Electronics and ECCE Asia (ICPE 2019 - ECCE Asia), Busan, South Korea, 2019, pp. 3059–3064. ISBN 978-1-7281-1612-9 https://doi.org/10.23919/ICPE2019-ECCEAsia42246.2019.8797051

[7] Xu, Y., Feng, X., Wang, J., Gao, C., Burgos, R., Boroyevich, D., Hebner, R. E. "Medium-Voltage SiC-Based Converter Laminated Bus Insulation Design and Assessment", IEEE Journal of Emerging and Selected Topics in Power Electronics, 7(3), pp. 1715–1726, 2019. https://doi.org/10.1109/JESTPE.2019.2922332

[8] Mehrabadi, N. R., Cvetkovic, I., Wang, J., Burgos, R., Boroyevich, D. "Busbar design for SiC-based H-bridge PEBB using 1.7 kV, 400 a SiC MOSFETs operating at 100 kHz", In: 2016 IEEE Energy Conversion Congress and Exposition (ECCE), Milwaukee, WI, USA, 2016, pp. 1–7. ISBN 978-1-5090-0738-7 https://doi.org/10.1109/ECCE.2016.7854903

[9] Srdic, S., Zhang, C., Lukic, S. "A low-inductance Sectional Busbar for Snuberless Operation of SiC-based EV Traction Inverters", In: 2019 IEEE Energy Conversion Congress and Exposition (ECCE), Baltimore, MD, USA, 2019, pp. 6805–6809. ISBN 978-1-7281-0396-9 https://doi.org/10.1109/ECCE.2019.8912204

[10] Singh, A. K., Pathak, M. K. "An Efficient Single-Stage Based Power Electronic Interface for Plug-in Electric Vehicles", IETE Technical Review, 37(2), pp. 169–179, 2020. https://doi.org/10.1080/02564602.2019.1584055

[11] Geng, C., He, F., Zhang, J., Hu, H. "Partial Stray Inductance Modeling and Measuring of Asymmetrical Parallel Branches on the Bus-Bar of Electric Vehicles", Energies, 10(10), 1519, 2017. https://doi.org/10.3390/en10101519

[12] Gui, H., Chen, R., Niu, J., Zhang, Z., Wang, F., Tolbert, L. M., Costinett, D. J., Blalock, B. J., Choi, B. B. "Design of Low Inductance Busbar for 500 kVA Three-Level ANPC Converter", In: 2019 IEEE Energy Conversion Congress and Exposition (ECCE), Baltimore, MD, USA, 2019, pp. 7130–7137. ISBN 978-1-7281-0396-9 https://doi.org/10.1109/ECCE.2019.8912605

[13] Chen, C., Pei, X., Shi, Y., Lin, X., Liu, X., Kang, Y. "Modeling and optimization of high power inverter three-layer laminated busbar", In: 2012 IEEE Energy Conversion Congress and Exposition (ECCE), Raleigh, NC, USA, 2012, pp. 1380–1385. ISBN 978-1-4673-0802-1 https://doi.org/10.1109/ECCE.2012.6342654

[14] Singh, P. B. T., Babu Bobba, P., Suresh, K., Varghese, B. J. "Extensive review on Laminated bus bar for low and high power applications", E3S Web of Conferences, 87, 01009, 2019. https://doi.org/10.1051/e3sconf/20198701009

[15] Grandvuillemin, J., Chamagne, D., Tiraby, C., Glises, R. "Ampacity of power bus bars for Hybrid-Electric or Electric Vehicles", In: 2008 IEEE Vehicle Power and Propulsion Conference, Harbin, China, 2008, pp. 1–6. ISBN 978-1-4244-1848-0 https://doi.org/10.1109/VPPC.2008.4677660

[16] Sharaf, A. M., Şahin, M. E. "A Flexible PV-Powered Battery-Charging Scheme for Electric Vehicles", IETE Technical Review, 34(2), pp. 133–143, 2017. https://doi.org/10.1080/02564602.2016.1155420

[17] Callegaro, A. D., Guo, J., Eull, M., Danen, B., Gibson, J., Preindl, M., Bilgin, B., Emadi, A. "Bus Bar Design for High-Power Inverters", IEEE Transactions on Power Electronics, 33(3), pp. 2354–2367, 2018. https://doi.org/10.1109/TPEL.2017.2691668

[18] Smirnova, L., Juntunen, R., Murashko, K., Musikka, T., Pyrhönen, J. "Thermal Analysis of the Laminated Busbar System of a Multilevel Converter", IEEE Transactions on Power Electronics, 31(2), pp. 1479–1488, 2016.
https://doi.org/10.1109/TPEL.2015.2420593

[19] Puigdellivol, O., Méresse, D., Le Menach, Y., Harmand, S., Wecxsteen, J.-F. "Thermal Topology Optimization of a Three-Layer Laminated Busbar for Power Converters", IEEE Transactions on Power Electronics, 32(6), pp. 4691–4699, 2017.
https://doi.org/10.1109/TPEL.2016.2601010

[20] Caponet, M. C, Profumo, F., De Doncker, R. W., Tenconi, A. "Low stray inductance bus bar design and construction for good EMC performance in power electronic circuits", IEEE Transactions on Power Electronics, 17(2), pp. 225–231, 2002.
https://doi.org/10.1109/63.988833

[21] Wang, J., Shaolin, Y., Zhang, X. "Effect of key physical structures on the laminated bus bar inductance", In: 2016 IEEE 8th International Power Electronics and Motion Control Conference (IPEMC-ECCE Asia), Hefei, China, 2016, pp. 3689–3694. ISBN 978-1-5090-1211-4
https://doi.org/10.1109/IPEMC.2016.7512886

[22] Zhu, X., Su, D., Zhang, Y., Wei, L. "Bus Bar Design for EMC Performance of Power Converters in Fuel Cell Electric Vehicles", In: 2006 IEEE International Conference on Vehicular Electronics and Safety, Shanghai, China, 2006, pp. 144–147. ISBN 1-4244-0758-3
https://doi.org/10.1109/ICVES.2006.371571

[23] Wen, H., Xiao, W., Li, H., Wen, X. "Analysis and minimisation of DC bus surge voltage for electric vehicle applications", IET Electrical Systems in Transportation, 2(2), pp. 68–76, 2012.
https://doi.org/10.1049/iet-est.2011.0035

[24] Chen, C., Pei, X., Chen, Y., Kang, Y. "Investigation, Evaluation, and Optimization of Stray Inductance in Laminated Busbar", IEEE Transactions on Power Electronics, 29(7), pp. 3679–3693, 2014.
https://doi.org/10.1109/TPEL.2013.2282621

[25] Wen, H., Xiao, W. "Design and optimization of laminated busbar to reduce transient voltage spike", In: 2012 IEEE International Symposium on Industrial Electronics, Hangzhou, China, 2012, pp. 1478–1483. ISBN 978-1-4673-0159-6
https://doi.org/10.1109/ISIE.2012.6237309